The Simulated Structure of Neutron Stars

Charles Smith

Student ID 9963262

Enrico Zammit Lonardelli

Student ID 9910821

ABSTRACT

Neutron stars were simulated by using the principle of hydrostatic equilibrium with Newtonian and general relativistic gravitational models. The star was built using the numerical method of the Runge-Kutta 4th order method, with both an ideal non-interacting Fermi gas and soft-core interacting equation of state. Radius and mass dependence on the equation of state used was investigated as well as the density structure of the stars for comparison against observations and predictions. Using the Tolman-Oppenheimer-Volkov equation, with Bethe & Johnson's equation of state, the maximum mass of a neutron star was found to be (1.78840 ± 0.00004) solar masses with radius (9.262 ± 0.002) km and the maximum radius was found to be (11.156 ± 0.002) km with mass (0.98280 ± 0.00004) solar masses.

1- INTRODUCTION

'It doesn't matter how beautiful your guess is, it doesn't matter how smart you are. If it doesn't agree with experiment, it's wrong'-Richard P. Feynman [1]. Neutron stars are perhaps one of the only loopholes in today's physics to this argument, we cannot experimentally validate the structure of neutron stars due to the extreme density conditions within. Observations made by various detectors are used to develop theory and equations of state. In this report neutron stars were simulated using numerical integration, the principle of hydrostatic equilibrium and two equations of state. The theorized matter distribution of compact stellar objects was analysed before examining the method of building the star. The equations of state used were based on neutron-neutron interactions (Bethe-Johnson) and a non-interacting fermi gas. We then aimed to show which of the equations of state tested best suits observation. Additionally, special relativistic rotation was added to the model as a fictitious force to give an approximate understanding of rotational effects to the structure of a star.

2- THEORY

2.1- STELLAR PROCESSES

If there was no opposing force to gravity, then there would only be gravitational singularities within the universe. Luckily for us, in our universe there tends to be an opposition to gravity in the form of kinetic effects such as radiation pressure due to the hydrogen and helium fusion process in main sequence stars, angular momentum (centrifugal) effects or magnetic/nuclear forces [2]. For white dwarves and neutron stars gravitational opposition is due to the Pauli exclusion principle which states that no two fermions may inhabit the same spatial co-ordinates, and since electrons and neutrons are both fermions degeneracy pressure is the force balanced against gravity [2]. There is a distribution of non-zero momentum for fermions at 0 Kelvin (cold matter), theoretically described by momentum space (k space) [3].

After a star can no longer sustain nuclear fusion and dissipates all other free energies opposing gravitational contraction on its own mass, it collapses onto its core. If the collapse is violent then some of the core mass may be expelled by the rebound of such a process [2]. If the core is less than 1.4 solar masses (M_S), fermi pressure in the form of electron degeneracy will oppose gravitation; this is a white dwarf star [4]. If the stellar core is more massive than the Chandrasekhar limit of $1.4M_S$, the electron degeneracy pressure will not stop the star from further collapse. Protons and electrons combine to produce neutrons and electron neutrinos, this also explains the neutrino flux detected from type-1A supernovae, leading to the formation of a degenerate fermi gas of neutrons. Baryonic fermi degeneracy will support the star from collapse; this is a neutron star. If the core is more than approximately $3M_S$ a black hole is formed (from the non-relativistic neutron approximation) [4].

2.2- THE THEORETICAL STRUCTURE

The structure of matter with varying density from a star's crust into its centre is fundamental to comparing observation to simulation. So, we formed a theoretical spherically symmetrical density distribution for our neutron star model.

On the surface/outer crust for densities less than $4.3x10^{14}kgm^{-3}$ a Coulomb lattice structure of neutron rich nuclei is formed, due to inverse beta decay enabled by the relativistic degenerate electrons. The nuclear binding energy peak representing the most stable nuclei will be slightly skewed by this effect. Beyond $4.3x10^{14}kgm^{-3}$ the inverse beta decay process becomes more prominent, causing the 'neutron drip', a process in which the neutron rich nuclei expel the neutrons into a neutron gas. Here, free electrons and neutrons co-exist in an equilibrium of superfluid gas. The neutron and electron gas with neutron rich nuclei can exist in this state up until the nuclear density of $2.3x10^{17}kgm^{-3}$. Interactions are very important between particles at densities above $2.3x10^{17}kgm^{-3}$. Past the nuclear density, the nuclei begin to merge, in a process called nuclear saturation, causing complex inter-nucleon interactions. This gives rise to a superfluid of electrons, neutrons and protons where baryonic/neutron degeneracy exerts an outward pressure due to the Pauli exclusion principle. At densities of the order $1x10^{18}kgm^{-3}$ the pressure may cause pion condensation; past this density, in extremely dense cores quark matter is hypothesised to be formed [5][6][7].

2.3- BUILDING A STAR

For a star not to collapse or explode each infinitesimally thin spherical shell of the neutron star matter must be in an equilibrium of pressures. The balance must be between the outward pressure caused by the degeneracy of the matter and the gravitational forces inward due to the mass inside that shell. This is the principle of hydrostatic equilibrium [8].

Using the Newtonian gravitational model, the pressure gradient and therefore condition for stellar equilibrium at radius r due to gravity is

$$\frac{dP}{dr} = \frac{-Gm(r)\rho(r)}{r^2} \qquad (1)$$

where $\rho(r)$is the density of matter at r, G is the universal gravitational constant and P is the pressure. The mass enclosed by a sphere of radius r ,$m(r)$ is given by the differential equation [8]

$$\frac{dm}{dr} = 4\pi r^2\rho(r) \qquad (2)$$

In Einstein's theory of gravitation, the corresponding condition for hydrostatic equilibrium is

$$\frac{dP}{dr} = \frac{-Gm(r)}{r^2}\frac{\left(1+\frac{P(r)}{\rho(r)c}\right)\left(1+4\pi r^3\frac{P(r)}{m(r)c}\right)}{\left(1-\frac{2Gm(r)}{rc^2}\right)} \qquad . (3)$$

Equation 3 [7] is called the Tolman–Oppenheimer–Volkoff equation (TOV). The TOV shows explicit pressure dependence on the pressure gradient leading to greater gravitational forces at a smaller mass than equation 1. Equation 3 was predicted by Oppenheimer and Volkoff in 1939 using a cold matter Fermi gas (one very similar to our non-interacting model in the following section). They found a maximum neutron star mass of 0.7 $M_s$using the TOV [9].

The above equations have been used with numerical integration and equations of state (EOS) to model neutron stars. We then compare the solutions of equations 1 and 3 and corresponding EOS's with observation.

2.4- The Equation of State

The equation of state describes the relation between the pressure and mass densities. In our models for simulations of neutron stars two equations of state were used, the Bethe-Johnson (BJ) and an ideal neutron gas EOS.

The Bethe-Johnson EOS [10] is a modified Reid soft core interaction model, using neutron-neutron (N-N) potentials to produce a repulsive core via meson exchange[6]. The BJ EOS uses Yukawa functions with parameters set to model experimental N-N scattering data [6]. The BJ EOS is

$$P(n) = 363.44n^{2.54} \quad (4.a)$$

$$\rho(n) = 236n^{2.54} + nm_n \quad , (4.b)$$

where n is the number density of neutrons, $P(n)$ is the pressure in $MeVc^{-2}fm^{-3}$and $\rho(n)$ is the density in $MeVc^{-2}fm^{-3}$. A conversion factor to SI units was applied to equation 4 before application in section 3. The BJ EOS is valid for the central density range of $(1.7 \times 10^{17} \leq \rho \leq 3.2 \times 10^{19})kgm^{-3}$ [6].

The ideal neutron gas EOS (NI) is the simplest model that can be used [5]. It is based on a non-interacting Fermi gas of neutrons. There are two parts to this equation of state; In the nonrelativistic regime the EOS is

$$P = \frac{\hbar}{5m_n^{\frac{8}{3}}}(3\pi^2)^{\frac{2}{3}}\rho^{\frac{5}{3}} \quad . (5.a)$$

The second part of the NI EOS in the relativistic approximation is given by

$$P = \frac{1}{3}\hbar c m_n^{\frac{-4}{3}}(3\pi^2)^{\frac{1}{3}}\rho^{\frac{4}{3}} \quad . (5.b)$$

The NI EOS is valid for $(0 \leq \rho \leq \infty)kgm^{-3}$[6], with the advised upper bound to be $(\rho \leq 5 \times 10^{17})kgm^{-3}$ due to the softening of the EOS relations due to N-N interactions. There is a critical density of value $\rho_c = 5 \times 10^{17}kgm^{-3}$ [11] specified for computational processes that acts as a bound between equations 5.a and 5.b. The value ρ_c is derived as an approximate figure using

$$\varepsilon_F = \frac{\hbar^2}{2m_n}\left(3\pi^2\frac{N}{V}\right)^{\frac{2}{3}} \ll E_{mn} \qquad (6)$$

[3], where ε_F is the Fermi energy of the neutron in this case, $\frac{N}{V}$ is the number of neutrons per unit volume in k space and E_{mn} is the rest mass of a neutron in joules. $\rho_c = 5 \times 10^{17} kgm^{-3}$ is the bound where equation 6 is no longer valid, in which the relativistic approximation is then used when above this density [5]. The maximum mass obtainable due to an ideal gas of degenerate neutrons is $5.8M_s$[7] and the maximum mass due to the TOV model dependant on the equation of state is between $3M_s$ and $5M_s$ [6].

We apply the BJ EOS central density region to comply simultaneously with both limits of the EOS's in the simulation described in section 3.1. Equations 4 and 5 will be used in conjunction with the differential equations in section 2.3 to simulate neutron stars. Both the BJ and NI equation of state assume a non-rotating neutron star.

3- COMPUTATIONAL METHOD

3.1- METHOD

The code for simulation was written in Python 3.5.3 using numerical integration as the base method to build a neutron star from a range of initial central densities. The primary numerical integration method used was the Runge-Kutta 4th order method (RK4). The computational method is outlined in Figure 1.

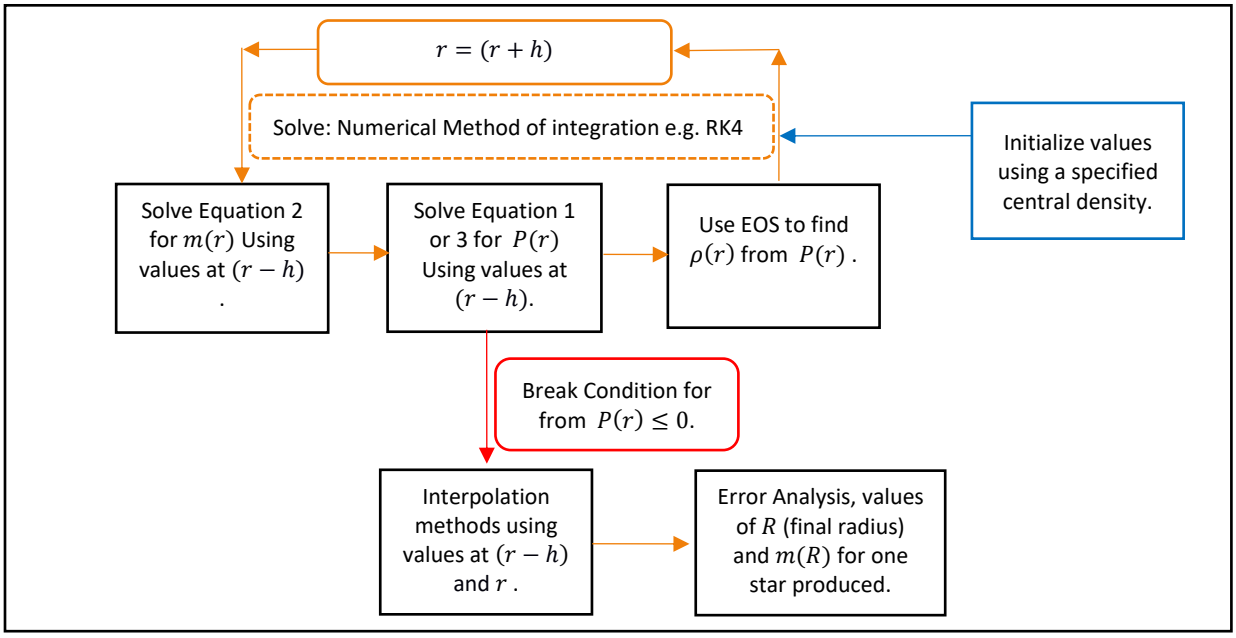

Figure 1: Computational method for a single central density.

Referring to Figure 1, a central density was initialised from the allowed limits. The central mass and radius were both initialized as zero [12]. A multistep numerical integration method was used until the program hit the break condition. The code then takes the last two points and interpolates using a linear fit and Newton Raphson to find the exact radius at which the pressure goes to zero. A linear fit was then applied to the respective masses and interpolation was used to find the final mass on the neutron star at the final radius.

The above method was implemented for a family of neutron stars, constrained by the BJ EOS central density limitations for comparative analysis against the NI EOS.

The BJ EOS central pressure was initialized by specifying the central density and using a Newton Raphson with equation 4. The NI EOS depends on two sub EOS's as mentioned in section 2.4. Therefore, when the program iterates through the numerical integration, decreasing in density until the critical density is reached (if the initial density is above the critical density), the EOS then changes from equation 5.b to 5.a as lower density regions are reached.

Plots of final mass vs final radius, central density vs final mass and central density vs final radius were all plotted. In addition, density/matter distribution graphs were plotted to show the internal structure on the star produced by their respective EOS and gravitational model.

Furthermore, Runge Kutta 5th order (RK5) and Euler numerical integration methods were implemented. The RK5 is mathematically more accurate than RK4 but with more numerical rounding error due to extra calculations in the code. The Euler method is mathematically less accurate than the RK4, but with only a single calculation it provides the least rounding error. These two methods provide an additional bound for our simulation result, with the RK4 chosen as the most suitable method for the primary results.

3.2- Errors

To calculate the errors on the mass and radius of the simulated neutron stars, two main elements of error were considered. The error in interpolation method is

$$E_{inter} = \pm(x_i - x_{i-1})^{n+1} \tag{7}$$

[13], where x_i , $x_{i-1}$are the respective points being interpolated and n is the order of polynomial, in our case this is linear and therefore $n = 1$. The error on the RK4 is calculated by simultaneously building the star with an RK4 that has a step size of twice that of the step size used for the result. The equation for the RK4 error is

$$E_{RK4} = \frac{|X_{2h} - X_h|}{(2^n - 1)} \tag{8}$$

[14], where X_h is the final value of numerical integration such as the mass or radius with single step of h and X_{2h} is the RK4 double stepped final value. Both the radius and the mass had both errors for equations 7 and 8 added in quadrature for their respective values.

3.3- Fictitious forces

The NI and BJ EOS's assume a non-rotating neutron star. To give a simple indication of what effect rotation would have on the structure of neutron stars, the pressure gradients of equations 1 and 3 were adapted to include the special relativistic centrifugal force on a shell of mass at a given radius [15].

4- Results and Discussion

4.1- Simulation Results

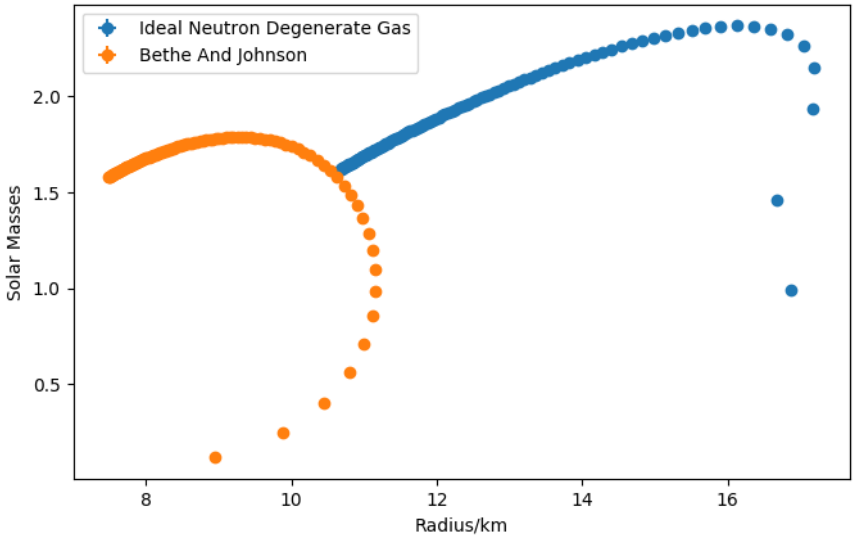

Figure 2: TOV Gravitational model, star mass against star radius displaying both EOS's from the central density limits.

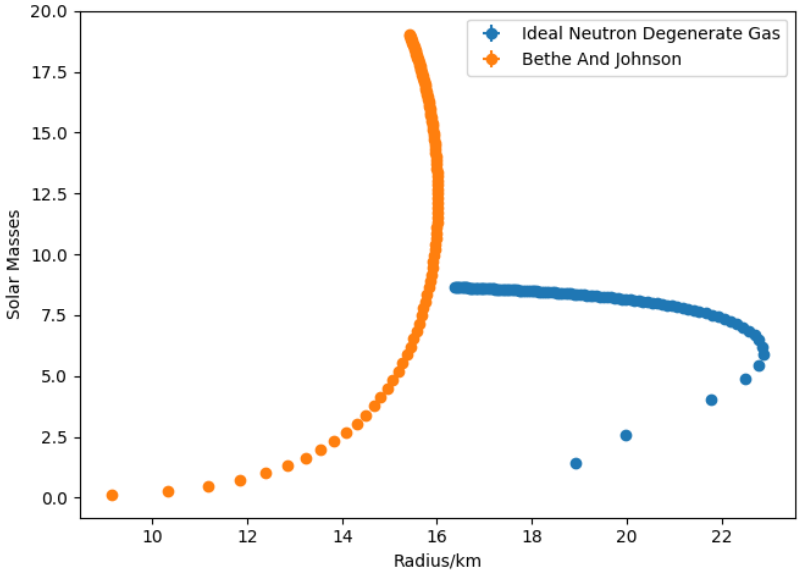

Figure 3: Newtonian Gravitational model, star mass against star radius displaying both EOS's from the central density limits.

Figures 2 and 3 compare the BJ and NI EOS's for the TOV and Newtonian model respectively. Figure 2 is under the TOV model for gravitation, the mass range for both EOS's fits limitations to the TOV model and is comparable to observed values [16]. These are masses between 1.3 M_s to 2.5 M_s and radii of about 10 kilometres. Figure 3 shows that the BJ EOS under the Newtonian model exceeds the maximum mass allowable by neutron degeneracy. The NI model under the Newtonian formalism still exceeds theoretical mass limit but fits more accurately to observation than that of the BJ EOS. Therefore, from above we conclude the general relativistic regime provides a more accurate model than Newtonian when compared to observation. This is as expected under the conditions of a relativistic system. We therefore provide results under the TOV model.

Our results show the maximum mass of a neutron star of the BJ EOS was found to be $(1.78840 \pm 0.00004)M_s$ with radius $(9.262 \pm 0.002)km$, the maximum radius was found to be $(11.156 \pm 0.002)km$ with mass $(0.98280 \pm 0.00004)M_s$ and the minimum mass was found to be $(0.1174 \pm 0.00004)M_s$ with radius$(8.9535 \pm 0.002)km$. The maximum mass of the NI EOS was found to be $(2.36860 \pm 0.00004)M_s$ with radius $(16.125 \pm 0.002)km$, the maximum radius was found to be (17.190±0.002) km with mass (2.15130±0.00004) M_s and the minimum mass was found to be $(0.9916 \pm 0.00004)M_s$ with radius $(16.8620 \pm 0.002)km$.

These results are also consistent with ones obtained from other theoretical models [17] that incorporate statistical analysis, numerous other equations of state, thermal dynamics and direct results from observation. The radius limit found using the BJ EOS does indeed lie in the $10\ km$ to $12\ km$ range stated by these theoretical models and with a maximum mass of $1.66M_s$ close to our value of $1.79M_s$ (obtained with the TOV combined with the BJ EOS).

The BJ and NI EOS hence fit well with current observations of neutron stars. The NI EOS fits very well with mass observations but does not with radius. This may be due to the assumption of a non-interacting neutron model or the critical density at which the relativistic NI EOS is implemented. Minimum bounds for the masses as part of our result due to TOV models are masses under the 1.4 M_s Chandrasekhar limit. We may observe neutron stars with masses slightly less than 1.4 M_s due to the star ejecting some of its own mass under gravitational collapse onto the neutron degenerate core as mentioned in section 2.1. The lower bound approximate limitation due to stellar evolution (Chandrasekhar limit) may explain the non-unique solutions seen in Figure 3 meaning that the lower mass solutions of a certain radius are just a product of the mathematical model and are unphysical. Both EOS's with the TOV remained within the neutron star mass limits of $3M_s$ to $5.8\ M_s$ after which a black hole then forms (Section 2).

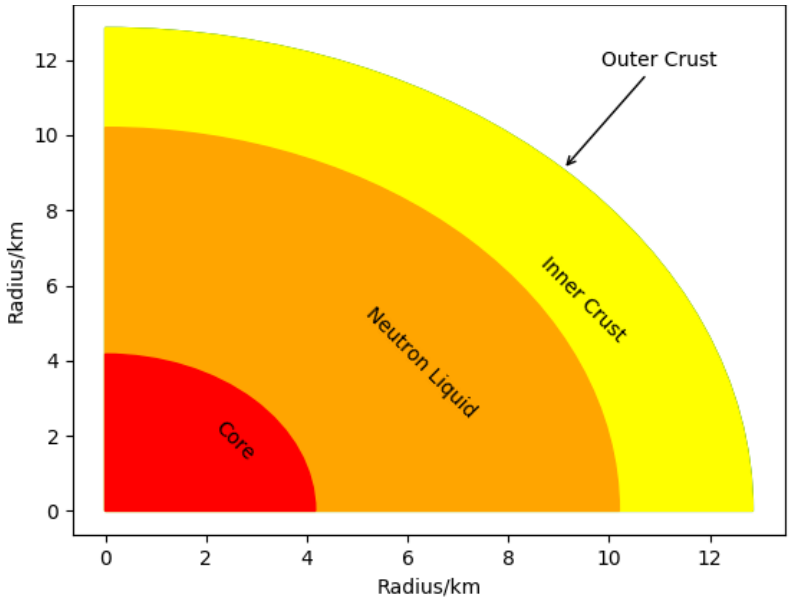

Figure 4: Density distribution model for NI EOS under the TOV model. Central Density: $3.669 \times 10^{17} kgm^{-3}$.

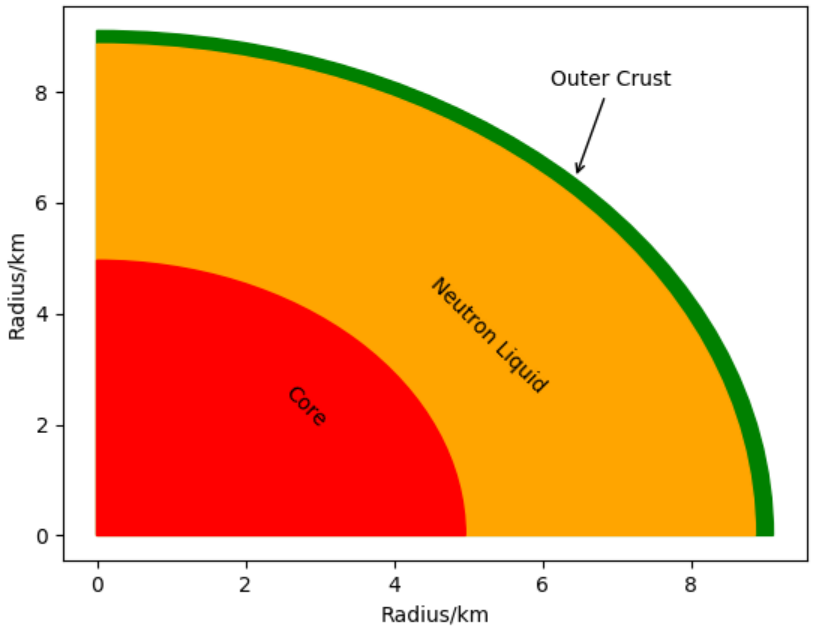

Figure 5: Density distribution model for BJ EOS under the TOV model. Central Density: $3.669 \times 10^{17} kgm^{-3}$.

Figures 4 and 5 provide an insight as to how the NI and BJ EOS's simulate the neutron star's internal structure under the TOV model for a specified central density. The core beyond the density of $1x10^{18}kgm^{-3}$: The BJ EOS has a slightly larger core than that of the NI EOS, this is due to the N-N interactions (and further hypothesized interactions such as pion condensation or quark matter) creating a more repulsive or soft core. As mentioned in section 2.2, at high densities interactions between particles play a much larger role in the EOS due to being over the nuclear saturation density. The neutron liquid region between $1x10^{18}kgm^{-3}$and $2.3x10^{17}kgm^{-3}$ is the point at which the EOS's begin to diverge in size. With the NI EOS having a much larger region than the BJ, this region is also around the point at which the NI EOS is changed from the relativistic to the non-relativistic approximation due to equation 6. The inner crust corresponds to the region of $2.3x10^{17}kgm^{-3}$ down to $4.3x10^{14}kgm^{-3}$where the BJ EOS has an extremely low proportion of its distribution within this region compared to the NI. The NI is most appropriate at this stage due to the lesser importance on N-N interactions when using the non-relativistic model. In the outer crust densities of less than $4.3x10^{14}kgm^{-3}$; the BJ has a larger region than the NI EOS showing that the BJ EOS's star surface is composed of a lattice structure whereas the NI EOS almost immediately is within the neutron drip region.

4.2- COMPUTATIONAL RESULTS

The results in section 4.1 were calculated using step sizes of 1 meter, Figure 6 shows how an increase in step sizes creates a divergence from the true numerical integration values, approximated by the 1-meter step size.

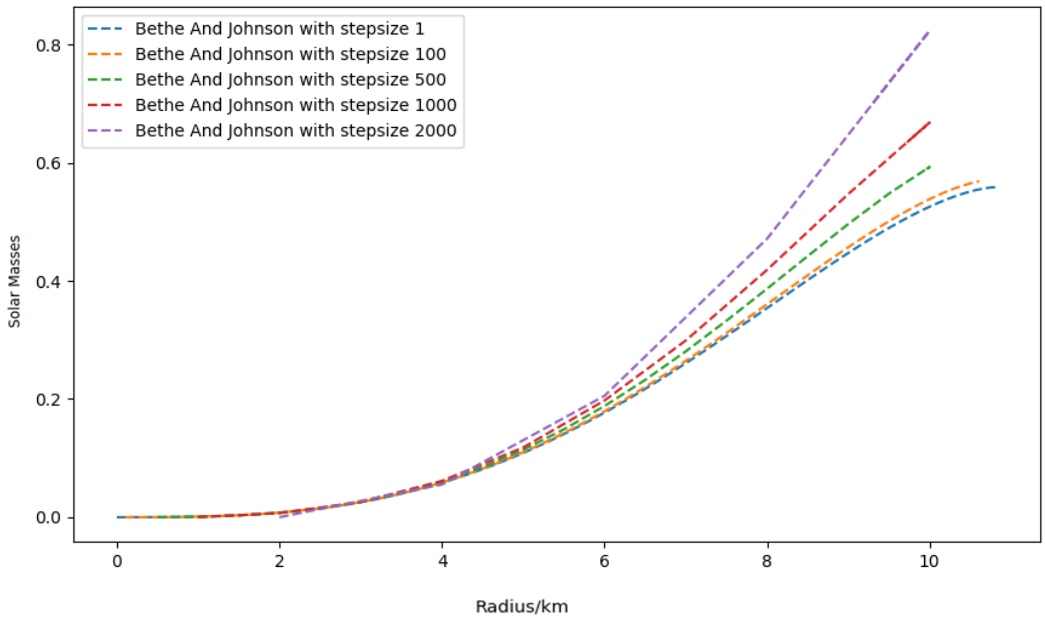

Figure 6: The effects of changing step size in meters with the RK4 integration method. The graph shows how an individual star is built with each step size.

The RK4 and Euler numerical integration methods were also run for the NI and BJ EOS's under the TOV model through the entire computational method, intended to give numerical bounds to our results above. Appendix-1A shows the resulting data comparison. For such a small step size of 1-meter relative size of a neutron star the RK4 and Euler method give similar values, whereas the RK5 always produced a larger value no matter the quantity. The RK5 at this point diverges due to numerical rounding error and therefore shows a disadvantage to using SI units instead of unitless variables and hence smaller numbers.

4.3- Rotational Effects

The effects of rotation using a special relativistic pressure gradient adaptation and a frequency of 641 Hz corresponding to one of the fasted observed neutron star rotations [18], Figure 7.

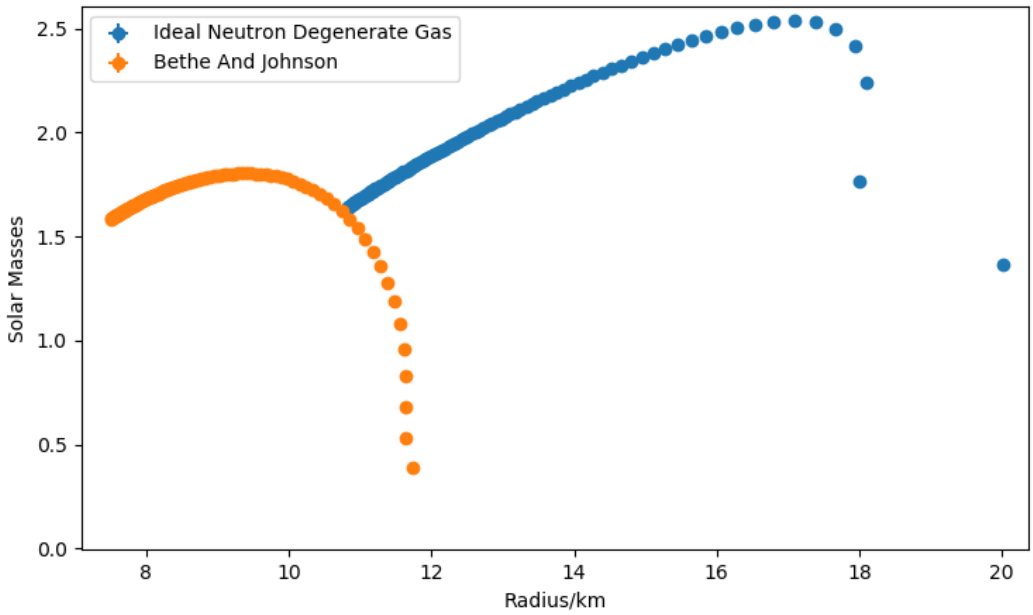

Figure 7: Rotational effects on a neutron star by modification of the pressure gradients in the TOV model.

Both EOS's and the TOV were used for this exercise. The change to the maximal mass and radius increase respectively for the NI EOS was approximately 6.72% and 14.17%. The increase to the maximal mass and radius increase respectively for the BJ EOS was approximately 1.04% and 5.1%. This shows an increase, although very small in comparison with the size of the star. The Newtonian model provides a similar result for rotation. More accurate calculations, such those using the Hartle–Thorne approximation [19], accounting for the oblate spheroid shape, Doppler boosts, and quadrupole moments of neutron stars giving a radial increase of approximately 4% for a 1.4 M_s star rotation at 600Hz [18], showing our indicative model gives the correct indication for rotational effects. We also see a distortion in the shape of the Mass/Radius plot, especially in the lower masses of stars when comparing Figures 2 and 7.

5- SUMMARY

The NI and BJ EOS's were compared across Newtonian and general relativistic regimes. The BJ EOS under the TOV gravitational model was found to be the most accurate when compared to current neutron star observations. This is due to the BJ EOS considering N-N soft core interactions unlike the NI EOS. The maximum mass of a neutron star of the BJ EOS was found to be $(1.78840 \pm 0.00004)M_s$ with radius$(9.262 \pm 0.002)km$. Neither EOS's with the TOV exceeded the neutron star mass limits of $3M_s$ to $5.8\ M_s$. The density distributions for the NI and BJ EOS's were analysed and the effects of rotation were explored showing an increase in maximum radius and mass for the EOS's. Multiple methods of integration were tested to give an additional bound to our results, this showed that for a more complex integration method unitless variables should be considered to avoid rounding error.

Additional investigations aimed at giving a more complete representation of a neutron star simulation could use different EOS's within the same integration for a singular star using critical densities as bounds between them to reflect the different types of interactions at varying densities. Additionally, more appropriate EOS's may be used when considering rotation.

APPENDIX - 1A

Integration Method	**RK5**	**RK4**	**Euler**
Maximum Mass (NI)	$2.6023\,M_s$	$2.3686M_s$	$2.3672\,M_s$
Maximum Mass Radius (NI)	$17.0342\ km$	$16.1247\ km$	$16.1250\ km$
Maximum Radius (NI)	$18.2221\ km$	$17.1901\ km$	$17.1945\ km$
Maximum Radius Mass (NI)	$2.3848\,M_s$	$2.1513\,M_s$	$2.1514\,M_s$
Maximum Mass (BJ)	$1.9329\,M_s$	$1.7884\,M_s$	$1.7868\,M_s$
Maximum Mass Radius (BJ)	$9.8616\ km$	$9.2616\ km$	$9.2640\ km$
Maximum Radius (BJ)	$11.8762\ km$	$11.1554\ km$	$11.1612\ km$
Maximum Radius Mass (BJ)	$1.1035\,M_s$	$0.9828\ M_s$	$0.9825\,M_s$

REFERENCES

[1] Pomeroy,R.S. The Key to Science (and Life) Is Being Wrong. [online] Available at: https://blogs.scientificamerican.com [Accessed 23 April 2018].

[2] Irvine, J. (1978). *Neutron stars*. Oxford: Clarendon Press, pp.1-12.

[3] Hook, J. and Hall, H. (2013). Solid state physics. Hoboken: Wiley, pp.52-82.

[4] Phillips, A. (2013). *The Physics of Stars*. Hoboken: Wiley, pp.30-31.

[5] Irvine, J. (1978). *Neutron stars*. Oxford: Clarendon Press, pp.115-131.

[6] Shapiro, S. and Teukolsky, S. (1983). *Black holes, white dwarfs, and neutron stars*. New York: Wiley, pp.188-294.

[7] Phillips, A. (2013). The Physics of Stars. Hoboken: Wiley, pp.171-204.

[8] Phillips, A. (2013). The Physics of Stars. Hoboken: Wiley, pp.5-10.

[9] Oppenheimer, J. and Volkoff, G. (1939). On Massive Neutron Cores. Physical Review, 55(4), pp.374-381.

[10] Bethe, H. and Johnson, M. (1974). *Dense baryon matter calculations with realistic potentials*. Nuclear Physics A, 230(1), pp.1-58.

[11] Creighton, J. (2012). *Relativistic Stars*. University of Wisconsin–Milwaukee.

[12] M.Hjorth-Jensen; *Computational Physics*; Available at: *http://folk.uio.no/mhjensen/computationalphysics.pdf* (2006) p289-293 [Accessed 16 March 2018].

[13] *Polynomial Interpolation: error analysis*. Available at: https://www.math.uh.edu/~jingqiu/math4364/interp_error.pdf [Accessed 21 March 2018].

[14] A.S.Chai. *Error estimate of a fourth-order Runge-Kutta method with only one initial derivative evaluation*. Hybrid Computer Laboratory, University of Wisconsin Madison.

[15] Jonsson, R. (2006). An intuitive approach to inertial forces and the centrifugal force paradox in general relativity. American Journal of Physics, 74(10), pp.905-916.

[16] Naeye,R, (n.d.). NASA - Neutron Stars. [online] Available at: https://www.nasa.gov/mission_pages/GLAST/science/neutron_stars.html. [Accessed 27 March 2018].

[17] Steiner,A.W et al (2010). The Equation of State from Observed Masses and Radii of Neutron Stars, The Astrophysical Journal,722(33), pp.49.

[18] Bauböck, M., Özel, F., Psaltis, D. and Morsink, S. (2015). ROTATIONAL CORRECTIONS TO NEUTRON-STAR RADIUS MEASUREMENTS FROM THERMAL SPECTRA. The Astrophysical Journal, 799(1), p.22.

[19] Chakrabarty, D., Morgan, E., Muno, M., Galloway, D., Wijnands, R., van der Klis, M. and Markwardt, C. (2003). *Nuclear-powered millisecond pulsars and the maximum spin frequency of neutron stars*. Nature, 424(6944), pp.42-44.